

Local regulation of pulmonary blood flow and ventilation-perfusion ratios in the coatimundi

B. J. B. GRANT, E. E. DAVIES, HAZEL A. JONES, AND J. M. B. HUGHES
Department of Medicine, Royal Postgraduate Medical School, Hammersmith Hospital, London W12 0HS, England; and Department of Physiology, Harvard School of Public Health, Boston, Massachusetts 02114

GRANT, B. J. B., E. E. DAVIES, HAZEL A. JONES, AND J. M. B. HUGHES. *Local regulation of pulmonary blood flow and ventilation-perfusion ratios in the coatimundi.* J. Appl Physiol. 40(2): 216-228. 1976—Small catheters (ca. 3 mm diam at tip) were wedged in subsegmental bronchi in anesthetized coatimundi (*Nasua nasua*) during spontaneous breathing. Mixed expired gases of a group of lobules were sampled continuously without contamination from neighboring units, and local tidal volume, frequency, carbon dioxide production, and oxygen consumption were measured, as well as mixed venous P_{O_2} and P_{CO_2} . Local ventilation-perfusion ratio, alveolar P_{O_2} , P_{CO_2} , and blood flow were calculated. There was a 22% reduction (range 15-38) in local perfusion (as percent of flow at $P_{A_{O_2}}$ 100 mmHg) per 10 mmHg fall in local alveolar oxygen tension over the $P_{A_{O_2}}$ range 150-36 mmHg. Local hypercapnia had little effect on local flow. Local tidal volume (ca. 1% of total tidal volume) was unaffected by changes in alveolar gas tensions. The contribution of vasoconstriction or vasodilatation, as a negative feedback system, to the stability of local $P_{A_{O_2}}$ was greatest close to the physiologic range (65-85 mmHg) falling off outside these values, but at best the system had only a moderate efficiency.

collateral ventilation; negative feedback; control systems; local ventilation; hypoxic pulmonary vasoconstriction; pulmonary gas exchange

IN 1946 VON EULER AND LILJESTRAND (9) found in the cat that breathing pure oxygen lowered pulmonary artery pressure and oxygen lack raised it. They postulated: "If the blood flow becomes inadequate in relation to the ventilation in some parts of the lungs, the corresponding alveolar air will become richer in oxygen and poorer in carbon dioxide. . . . This will lead to a dilatation of the blood vessels of that part of the lungs. Oxygen want and carbon dioxide accumulation call forth a contraction of the lung vessels, thereby increasing the blood flow to better aerated lung areas, which leads to improved conditions for the utilization of the alveolar air." Following extensive research in the next decade constriction of pulmonary blood vessels in response to breathing low oxygen mixtures (10-12%) was shown in every species in which it was tested (11). This approach did not exclude the possibility that pulmonary vasoconstriction may have been caused by systemic hypoxia rather than alveolar hypoxia. Studies in various species including conscious man showed that unilateral hypoxia intro-

duced by means of a tracheal divider or Carlens tube caused a redistribution of pulmonary blood flow away from the hypoxic lung (1, 20) even when systemic arterial desaturation was avoided by breathing 100% oxygen in the other lung (17). In open-chest anesthetized dogs and cats Barer et al. (3) confined hypoxia to the lower lobe and found an increase in local vascular resistance. Nevertheless the von Euler-Liljestrand hypothesis had still not been tested at a sublobar level, nor had the implications of local pulmonary vasoconstriction in terms of alveolar gas exchange been explored.

The purpose of our present study was to determine whether local alveolar hypoxia reduced local pulmonary blood flow in much smaller lung units and to what degree this mechanism might improve local gas exchange. This is of practical importance since the majority of lung disease affects lung units smaller than a lobe.

The advantage of confining hypoxia or hyperoxia to small segments of lung is that the part played by systemic mechanisms (such as alterations in mixed venous or arterial blood composition) will be negligible compared to local effects. Local vascular responses in the intact lung have not previously been studied, and this paper describes a new method.

In some mammals, such as the sheep, the interlobular fibrous septa are unusually well developed so that the lungs lack the communications which permit collateral airflow between subsegments of a lobe. This is true for *Nasua nasua*, the coatimundi (J. Mead and D. Leith, personal communication). Coatis are small mammals from Central and South America of the family Procyonidae. They are convenient for a laboratory study because of their size (2-5 kg body wt). By wedging a catheter in a group of lobules within a lobe, mixed expired gas was sampled without contamination from neighboring units. Since the tidal volume of the lobules was only a small fraction of that for the lung as a whole (about 1%), local hypoxia or hyperoxia could be produced without any changes in the systemic circulation or overall ventilation while the animal was breathing spontaneously with minimum operative interference. From the respiratory exchange ratio of the mixed expired gas, the mixed venous blood and inspired gas compositions we calculated the local ventilation-perfusion ratio and alveolar oxygen and carbon dioxide tensions as described by Rahn (27) and Riley and Cournand (31), and solved the

Fick equation indirectly for local blood flow and alveolar ventilation.

METHODS

Experimental Arrangement

Thirteen coatis were studied weighing between 1.8 and 5.5 kg. Anesthesia was induced intraperitoneally with 1% chloralose and 10 or 20% urethan in a dose of 4–7 mg/kg body wt and was maintained throughout the experiment with chloralose alone. After tracheostomy, a jugular venous catheter (0.86 mm ID, 1.27 mm OD) was inserted with its tip in the right atrium for mixed venous blood sampling and a femoral catheter (0.76 mm ID, 1.22 mm OD) for arterial blood sampling. An esophageal balloon (5 cm length and 0.5 ml operating volume) was passed for monitoring esophageal pressure. The animal was breathing spontaneously throughout the experiment in a body plethysmograph (Fig. 1). Tidal volume was measured by plethysmograph volume displacement using a Krogh spirometer (Emerson Co., Mass). Rectal temperature was measured with a thermometer; the animal was warmed with a heating pad. A metal cannula (volume 68 ml) was attached to the tracheostomy; air was supplied into the tracheal end of the cannula at a flow rate between 0.7 and 1.0 l/min to reduce instrumental dead space. A catheter (1.9 mm OD, 1.4 mm ID) was wedged in a small airway subtending a group of lobules. The tip of the catheter was bell-shaped (2.9–3.5 mm diam) to reduce the chance of obstructing the bronchi branching off proximally. The instrumental dead space was eliminated by delivering a bias flow of gas through fine polyethylene tubing (0.28 mm ID, 0.66 mm OD) lying within the lobular catheter. The resistance of the bronchial catheter with the inner catheter inside it was $0.1 \text{ cmH}_2\text{O}\cdot\text{ml}^{-1}\cdot\text{min}$.

The experimental arrangement for the lobule¹ is set out in detail in Fig. 2. Inspiratory or bias gas was delivered from a gas cylinder through a series of reducing valves. A short segment of high-resistance metal tubing was interposed upstream and flow rate was monitored with a Sanborn 267B pressure transducer; for the flow rates used, the pressure-flow relations in the tubing were linear.

The lobule was connected via the bronchial catheter to a purpose-built miniature Krogh spirometer with which tidal volume was recorded. It must be emphasized that the catheterized segment was free to ventilate spontaneously; its tidal volume followed the same pattern as that of the rest of the lung. When deep breaths or sighs, apneic pauses, etc., were noted in the lung ventilation pattern, these were always reflected in the recordings of lobule tidal volume. Ideally, the specific tidal volumes of lung and lobule would have been equal but measurements of the respective volumes were not available to check this. Without the bias flow of gas the lobule would merely have rebreathed the instrumental dead space and its "effective" ventilation would have

¹ For convenience we use the words "lobular unit" and "lobule" interchangeably although a group of secondary lobules (up to 10) was in fact studied.

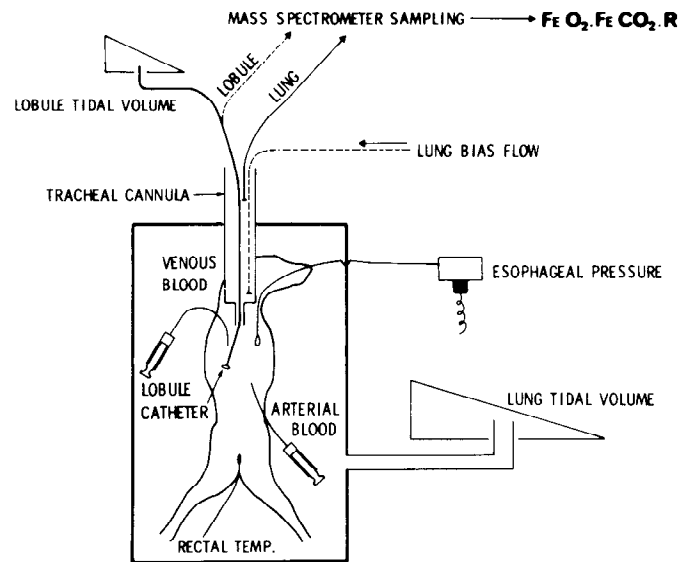


FIG. 1. Diagram of experimental conditions with coati in a body plethysmograph. A cannula was attached to the tracheostomy opening and a small catheter passed and wedged in a peripheral lung unit. Mixed expired oxygen and carbon dioxide fractions from lung and "lobule" were analyzed with a mass spectrometer and expiratory exchange ratios (R) calculated. A bias flow ($500\text{--}800 \text{ ml}\cdot\text{min}^{-1}$) was introduced into the tracheal cannula to overcome dead space.

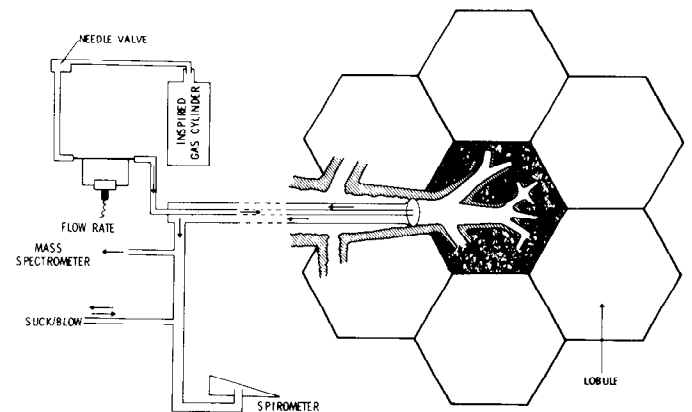


FIG. 2. Schema to show gas inflow and outflow from lobular unit. Inspired gas reached the unit through a fine catheter within the lobule catheter. Flow rate was controlled by a needle valve and monitored from the pressure drop across a section of narrow metal tubing. Suck/blow system added or subtracted (via needle valves) a constant flow of gas, equal but opposite to the inspired gas minus mass spectrometer sampling rate, in order to keep the spirometer tidal volume record on scale.

been nil. As Fig. 2 shows, the bias flow of inspired gas passed out of the inner catheter at the tip of the bronchial catheter and flowed back along the outer catheter becoming mixed expired gas because a certain fraction has exchanged with the lobule to become alveolar gas. This bias flow system enabled us to vary the "effective" ventilation of the lobular unit, from close to zero when the flow was minimal up to, at high flow, a maximum which was set by the actual minute ventilation of the lobular unit minus its own dead space. These changes of "effective" ventilation, which could be achieved without any changes in tidal volume, were analogous to changes of dead space-to-ventilation ratio.

Changes of alveolar gas tensions were achieved in one

of two ways: 1) by changing anatomic dead space and "effective" ventilation as just described, or 2) by changing the composition of the inspired gas without altering the bias flow rate.

To record the actual minute ventilation and tidal volume of the lobules, the spirometer level was kept constant by adding and subtracting gas from the system with high-precision needle valves. By closing the suck/blow line and mass spectrometer sampling line, the rate of accumulation of mixed expired lobular gas in the miniature spirometer should equal inspired gas flow, as monitored upstream. This provided the most convenient method of checking during the course of the experiment that the lobular catheter was wedged and the system free from leaks. The lobular bias flow and tidal volume, esophageal pressure, and lung tidal volume were recorded on a direct-writing Hewlett-Packard 7700 recorder.

Measurement of Inspired and Expired Gas Fractions and Respiratory Exchange Ratio

The mixed expired gas from the lobules was sampled continuously at a flow rate of 1.38 ml/min using a mass spectrometer (modified MS4, AE1, England). The mass spectrometer (MS) was linked to a small on-line computer (Digico) giving direct printout of averaged values over each 6- or 7-s period of oxygen and carbon dioxide fractions, and respiratory exchange (gas R) ratio, calculated from the equation (26)

$$R = \frac{(1 - FI_{O_2}) FE_{CO_2} - (1 - FE_{O_2}) FI_{CO_2}}{(1 - FE_{CO_2}) FI_{O_2} - (1 - FI_{CO_2}) FE_{O_2}} \quad (1)$$

where FI_{O_2} and FI_{CO_2} are inspired oxygen and carbon dioxide fractions and FE_{O_2} and FE_{CO_2} are mixed expired oxygen and carbon dioxide fractions.

The digital computer was programmed to constantly divide individual partial pressures by the summed total of all partial pressures (O_2 , CO_2 , N_2 , argon) to obtain the fractional dry gas composition. In this way sampling errors common to all gases, i.e., caused by variation in the pressure balance in the inlet system of the MS, are avoided and an accuracy of ± 1 mmHg for PO_2 and PCO_2 is maintained (5). Changes in MS sensitivity, other than those due to sampling errors, were checked with calibrating gases and with air. Because of the higher concentrations, changes in sensitivity to oxygen have more effect on the accuracy of the gas R calculations. Therefore the lobule inspired gas, usually air from a cylinder, was sampled as frequently as the protocol allowed. A 1% change in sensitivity for oxygen would lead to a 5% error in calculation of inspired-expired oxygen difference and gas R; in practice we never observed sensitivity changes greater than 0.2%.

An example of the on-line computer output is shown in Fig. 3 with lobule inspired gas sampled as a reference before the measurements of mixed expired gas. The computer "clock" provided a time signal, recorded in binary form on the four-channel recorder, so that lobule ventilation and inspired gas flow could be matched with gas R measurements. A lag time, of approximately 20 s but dependent on inspired flow rate, between measure-

O_2	CO_2			
20.80	0.06	REF.		
20.83	0.06	REF.		
20.83	0.06	REF.		
20.88	0.06	REF.		
RUN.				
FE_{O_2}	FE_{CO_2}	R	MIN	SEC
17.31	2.29	0.583	15	47
17.43	2.21	0.581	15	54
17.50	2.17	0.584	16	0
17.62	2.13	0.597	16	6
17.76	2.04	0.597	16	13
17.79	2.04	0.602	16	19
17.70	2.01	0.575	16	25
17.79	2.01	0.594	16	32
17.75	2.03	0.590	16	38
17.77	2.03	0.596	16	45
17.81	2.01	0.596	16	51
17.74	2.00	0.580	16	57
17.85	1.97	0.592	17	4
17.98	1.88	0.590	17	10
18.29	1.71	0.602	17	16
17.88	1.90	0.575	17	23
17.97	1.87	0.584	17	29
18.05	1.83	0.588	17	35

FIG. 3. Example of on-line computer output from mass spectrometer sampling. After sampling the inspired (i.e., reference (REF) gas), sampling line was switched (RUN) to mixed expired gas from lung or lobule. Fractional concentrations of mixed expired oxygen (FE_{O_2}) and carbon dioxide (FE_{CO_2}) and respiratory exchange ratio (R) were recorded over 6- or 7-s periods. Normal fluctuation of these values is shown for steady-state sampling from the lobule over a 2-min period.

ments of R and of ventilation or flow was allowed for. For the calculation of \dot{V}_A/\dot{Q} and alveolar gas tensions in the steady state, values of R, FE_{O_2} , and FE_{CO_2} were averaged over 1-min periods.

Measurement of Blood Gas Tensions

During each experiment, arterial and mixed venous blood samples were analyzed periodically for pH, carbon dioxide, and oxygen tensions using electrodes (Blood Microsystem, Radiometer, Copenhagen) and an acid-base analyzer (PHM71). The volume of blood removed for these measurements had to be minimized in view of the size of the animals. Blood (0.5 ml) was taken into capillary tubing after clearance of catheter dead space. Blood gas tensions were measured immediately after sampling. Only single estimates could be made on each sample. For oxygen tension, a correction was made for the difference (7%) between the electrode reading with gas compared with tonometered blood. Corrections for body temperature were included in the off-line computer program; in two experiments, temperature was not measured and was assumed to be 37°C. During the course of an experiment, three to five samples of mixed venous blood were obtained. Over several hours, the values for mixed venous blood gas tensions and pH at any particular time were interpolated.

Other Measurements

The tidal volume of the group of lobules ranged between 0.4 and 1 ml whereas the tidal volume of the lungs ranged between 60 and 80 ml. Because such a small proportion of the lung was studied (approximately 1%), its contribution to gas exchange was small; changes in lobule alveolar gas composition had no dis-

cernible effect on the systemic blood gas composition or total ventilation. Hemoglobin concentrations and hematocrit were also measured. In the last eight experiments, estimates of oxygen content were made using a saponin/potassium ferricyanide method (23) and an oxygen electrode (Radiometer type EJ044).

At the end of each experiment, the lungs were examined macro- and microscopically and the position of the lobular catheter was found to be in the left or right lower lobe. The lungs were normal apart from one experiment where albumin macroaggregates had been injected for assessment of regional perfusion prior to death and multiple petechial hemorrhages were found. The lung subtended by the lobular catheter was normal in every case; there was no local edema.

Calculation of Results

The derivation of blood flow (\dot{Q}), alveolar oxygen tension ($P_{A_{O_2}}$), and ventilation-perfusion ratio (\dot{V}_A/\dot{Q}) for the lobule was based on the calculation of "ideal alveolar" P_{O_2} and P_{CO_2} using the measured values for mixed venous P_{O_2} and P_{CO_2} , inspired oxygen and carbon dioxide fractions ($F_{I_{O_2}}$ and $F_{I_{CO_2}}$), the respiratory exchange ratio in mixed expired gas (gas R), and the O_2 - CO_2 diagram (31). The principal steps are set out schematically in Fig. 4 as boxes joined by continuous lines, and an alternative method used when hypoxic or hypercapnic inspired gas mixtures were used is shown in interrupted lines. For clarity the main steps in the analysis will be outlined.

1) The input data consisted of hemoglobin concentration, hematocrit, rectal temperature, barometric pressure, inspired ($F_{I_{O_2}}$, $F_{I_{CO_2}}$) and mixed expired ($F_{E_{O_2}}$, $F_{E_{CO_2}}$) oxygen and carbon dioxide fractions, mixed venous pH and gas tensions, ($P\bar{v}_{O_2}$, $P\bar{v}_{CO_2}$), inspired (bias) gas flow rate, and gas R.

2) Mixed venous oxygen ($C\bar{v}_{O_2}$) and carbon dioxide ($C\bar{v}_{CO_2}$) contents were calculated from $P\bar{v}_{O_2}$ and $P\bar{v}_{CO_2}$ using the dissociation curves. $C\bar{v}_{O_2}$ was calculated with the function suggested by Gomez (14) for the cat whose P_{50} is 36.5 mmHg. The P_{50} , corrected to pH 7.4 and 37°C, of coati blood in two animals has been found to be 37

mmHg (A. J. Bellingham, personal communication) which was in agreement with our measurements of contents and tensions measured during the course of the experiments. Oxygen capacity, measured in tonometered blood from three animals, was 1.33 ml oxygen/g hemoglobin. The Bohr effect, in two animals, was -0.28 ($\Delta \log_{10} P_{50}/\Delta pH$).

3) The calculation of "ideal alveolar" P_{O_2} and P_{CO_2} was performed with an off-line computer program suggested by Kelman (20). In brief an iterative method is used, choosing successive values of alveolar gas tensions compatible with the measured gas R until the blood R $[(C\bar{v}_{CO_2} - Cc'_{CO_2})/(Cc'_{O_2} - C\bar{v}_{O_2})]$ calculated from these values was within ± 0.001 of the gas R. For this purpose ideal alveolar and end-capillary P_{O_2} and P_{CO_2} were assumed to be equal; Cc'_{O_2} and Cc'_{CO_2} were calculated from the dissociation curves.

4) \dot{V}_A/\dot{Q} ratio was calculated as $8.63 (C\bar{v}_{CO_2} - Cc'_{CO_2}) \cdot (1.0 - F_{I_{O_2}} - F_{I_{CO_2}})/P_{A_{CO_2}} (1 - F_{I_{O_2}})$.

5) CO_2 output (\dot{V}_{CO_2}) = $F_{E_{CO_2}} \cdot \dot{V}_I$, where \dot{V}_I was inspired (bias) gas flow rate.

6) The Fick equation for blood flow—indirect Fick since O_2 and CO_2 contents were calculated from tensions—was calculated in the usual manner, and alveolar ventilation (\dot{V}_A) as $(\dot{V}_A/\dot{Q})/\dot{Q}$. Gas R was also measured from the trachea, and in experiments 7 and 8 total CO_2 production as well. Total pulmonary blood flow was calculated as described for the lobule.

Oxygen tensions and contents could have been substituted for CO_2 in the measurements of \dot{Q} and \dot{V}_A/\dot{Q} because all measurements are linked by the gas and blood R ($\dot{V}_{CO_2}/\dot{V}_{O_2}$). With $F_{I_{O_2}} < 0.105$ and $P_{I_{CO_2}} > P\bar{v}_{CO_2}$ an alternative method of calculation was employed (Fig. 4, interrupted lines), the reasons for which are given in the section B-8 in CRITICISM OF METHODS. \dot{V}_{CO_2} was calculated in the usual way and \dot{V}_{O_2} solved as R/\dot{V}_{CO_2} . A value of alveolar ventilation was chosen on the basis of values obtained immediately before and after the hypoxic/hypercapnic period when the lobule inspired gas was air. Since there were little or no changes in total ventilation or tidal volume of the lobule throughout this period, this assumption appeared justified, granted that

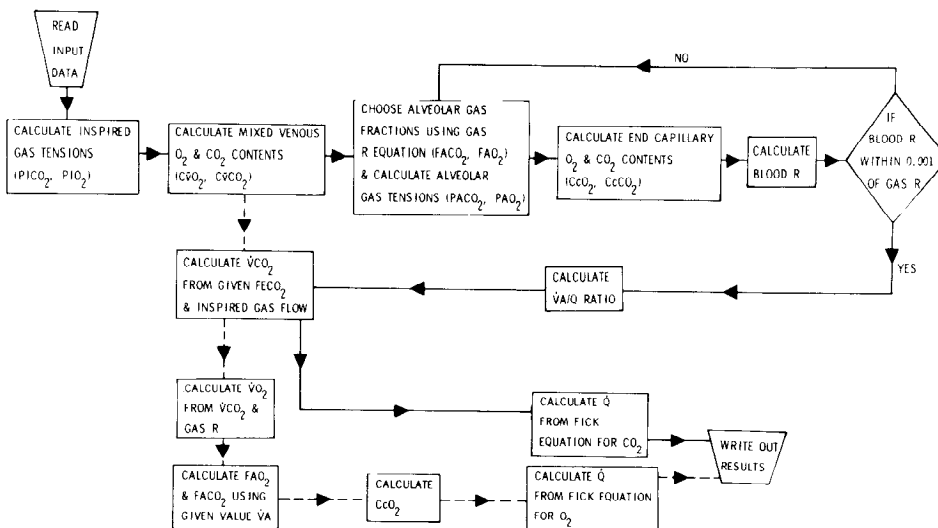


FIG. 4. Flow chart showing the calculation of local alveolar gas tensions and local blood flow. Solid lines indicate the sequence used in the off-line computer program when lobular inspired gas was air. Because of the constraint that blood R approximates to gas R, the Fick equation for either CO_2 or O_2 can be used for the calculation of local blood flow. Interrupted lines indicate the calculation for hypoxic and/or hypercapnic inspired gas. Values of alveolar ventilation were chosen from those calculated breathing air immediately before and after the measurement (total ventilation being similar). Note that with this method of calculation the constraint that blood R approximates to gas R, no longer applies.

no significant changes in lobule dead space occurred. Mean alveolar oxygen and carbon dioxide fractions (FA_{O_2} , FA_{CO_2}) were calculated from $\dot{V}CO_2$ or $\dot{V}O_2$ and \dot{V}_A , and end-capillary contents derived from dissociation curves. The Fick equation (using oxygen) was then used to calculate blood flow.

RESULTS

Thirteen animals were studied. The first five were pilot experiments with measurements of gas R only. Body and lung weights in the second series of eight animals are given in Table 1. *Animals 1 and 6* died prematurely before the lobule catheter was properly positioned and stable conditions were not achieved in *animal 4*. Except for the mixed venous P_{O_2} and P_{CO_2} , the range of values within any experiment was too small to be recorded in Table 1 and the mean is given. Table 2 records the range of values for respiratory exchange ratio (R), tidal volume, and frequency for lung and lobules, dynamic lung compliance, and arterial blood gas tensions. The range of R values for the lobules includes the effect of changes of inspired flow rate.

Effect of Changing Lobule Inspired Gas Composition

Figure 5 presents direct observations of oxygen consumption ($\dot{V}O_2$), carbon dioxide production ($\dot{V}CO_2$) and minute ventilation (\dot{V}_E) in the lobules of *experiment 8* as their inspired oxygen fraction was varied from zero to 0.3. Respiratory exchange ratio (R) increased from 0.35 at FI_{O_2} 0.31 to 3.26 at FI_{O_2} 0.076 becoming negative (-1.4

TABLE 1. Coatimundi body and lung weight, mean hemoglobin, hematocrit, rectal temperature, mixed venous pH, and range of mixed venous oxygen and carbon dioxide tensions

Animal No.	Body Wt, kg	Lung Wt, g	Hb, g/100 ml	Hct %	T_{re} , °C	pH _i	Pv_{O_2} , mmHg	Pv_{CO_2} , mmHg
2	4.83	29.5	16.2	44.1	37.0	7.30	43-41	45-43
3	3.60	41.0	14.7	44.2	37.0	7.29	41-31	49
5	3.18	34.0	11.5	36.2	38.9	7.37	58-51	40-29
7	5.50	26.0	13.1	41.0	40.0	7.35	32	34-33
8	4.05	23.8	19.0	49.8	39.2	7.40	46-37	39-22
Mean	4.23	30.8	14.9	43.1	38.5	7.34	44-38	41-35

Hb = hemoglobin; Hct = hematocrit; T_{re} = rectal temperature; pH_i = mixed venous pH; Pv_{O_2} and Pv_{CO_2} = mixed venous oxygen and carbon dioxide tensions.

TABLE 2. Range of respiratory exchange ratio and tidal volume for whole lung and lobules studied, respiratory frequency, dynamic lung compliance, arterial oxygen and carbon dioxide tensions

Expt. No.	R (lung)	R (lobule)	V_T (lung), ml	V_T (lobule), ml	f , min^{-1}	C_{dyn} , $ml \cdot cmH_2O^{-1}$	Pa_{O_2} , mmHg	Pa_{CO_2} , mmHg
2	0.67-0.76	0.56-0.87	76-80	0.32-0.42	10-13	31-32	83-85	36-35
3	0.75-0.77	0.47-0.61	14-20	0.26-0.34	14-17	4-6	87-90	38-40
5	0.63-0.73	0.61-0.90	60-80	0.12-0.20	21-82	18-24	94-102	35-24
7	0.67-0.75	0.58-0.79	68-93	0.20-0.32	16-20	20-21	92-96	27-22
8	0.69-0.78	0.48-0.57	56-84	0.32-0.44	9-15	21-24	102-109	35-20
Mean of lowest and highest	0.68-0.76	0.54-0.77	55-71	0.24-0.34	14-29	19-21	91-97	33-27

All measurements made with animals breathing air. R = respiratory exchange ratio; V_T = tidal volume; f = respiratory frequency; C_{dyn} = ΔV_T (lung)/ Δ esophageal pressure; Pa_{O_2} and Pa_{CO_2} = arterial oxygen and carbon dioxide tensions.

to -2.05) at FI_{O_2} of zero. A negative $\dot{V}O_2$ and R occurred when pure nitrogen was inspired since lobule inspired oxygen concentration was less than Pv_{O_2} . There was a systematic fall in lobule $\dot{V}O_2$ and $\dot{V}CO_2$ but no significant change in lobule total ventilation. These data strongly suggest that local blood flow is related to local oxygen tension unless gross and wholly uncharacteristic changes in the distribution of ventilation and perfusion occurred within the lobular unit. Changes in local blood flow and \dot{V}_A/Q ratio were calculated from these data as shown in Fig. 6. Effectively local flow falls to close to zero at PA_{O_2} 40 mmHg. At PA_{O_2} 13 and 8 mmHg local flow was 0.55 and 0.32 $ml \cdot min^{-1}$ but these results have not been shown in the figure nor included in the regression line equation. The linear relationship between local perfusion and alveolar P_{O_2} over such a wide range (P_{O_2} 40-150 mmHg) is of great interest and hitherto unreported.

In this experiment, the effect of hypercapnia on local perfusion was tested under normoxic and hypoxic conditions. As shown in Fig. 7, there was no significant change in local blood flow under hypercapnic conditions.

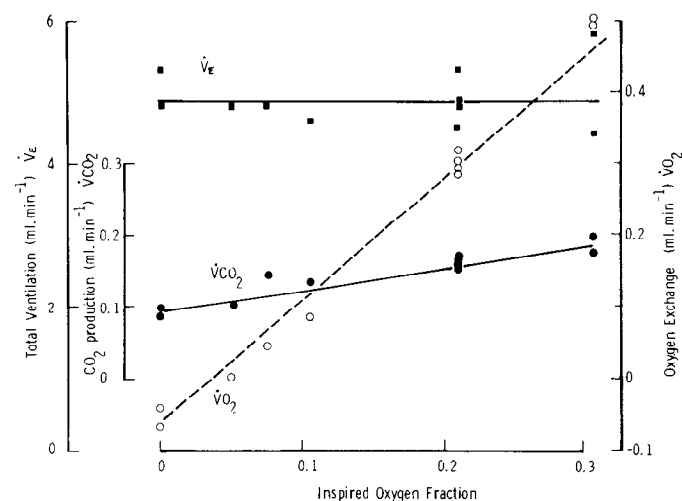


FIG. 5. *Experiment 8a*. Effect of changes of inspired oxygen concentration (FI_{O_2}) on minute ventilation (BTPS), oxygen exchange ($\dot{V}O_2$), and carbon dioxide output ($\dot{V}CO_2$) at STPD for a group of lobules. Changes of inspired oxygen fraction were made in the following order 0.21, 0.31, 0.076, 0.21, 0.0, 0.21, 0.31, 0.10, 0.05, 0.21. Mixed venous P_{O_2} 46-44.5 mmHg, P_{CO_2} 39-32 mmHg, pH 7.38-7.39. Note negative oxygen exchange at zero inspired oxygen and 50% fall in $\dot{V}CO_2$ at constant ventilation. Calculated regression lines shown.

Effect of Changing Lobule Alveolar Ventilation

In experiments 2-5, local $P_{A_{O_2}}$ was changed by altering local alveolar ventilation rather than the composition of the inspired gas. Alveolar ventilation was changed by varying the inspired gas flow rate. In effect, this maneuver altered the anatomical dead space-to-tidal volume ratio of the lobule. We subsequently found

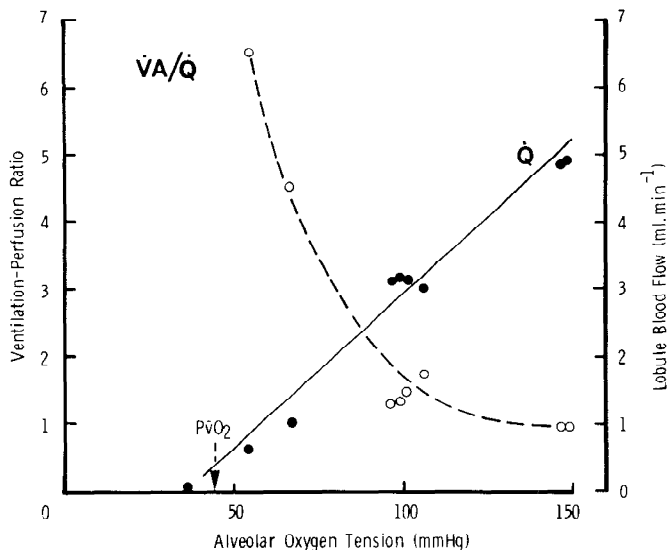


FIG. 6. Data of Fig. 5 replotted as lobule blood flow (Q) and ventilation-perfusion (\dot{V}_A/Q) ratio against local alveolar oxygen tension ($P_{A_{O_2}}$). Continuous line is calculated regression of Q on $P_{A_{O_2}}$ over the range 40-150 mmHg. Arrow indicates mixed venous oxygen tension (Pv_{O_2}).

that the range of $P_{A_{O_2}}$'s produced in this way was rather limited. Nevertheless, it is a truly physiological disturbance compared to changes in inspired gas composition. Additionally, the extent to which the pulmonary circulation could control local P_{O_2} breathing air could be directly studied.

Figure 8 shows, in detail, one example of the effect of changes in alveolar ventilation on local blood flow, \dot{V}_A/Q ratio, and alveolar P_{O_2} . Changes in inspired gas flow were made at times indicated by arrows in the figure and were complete in 0.3 min as recorded upstream from the lobule. The time constant of the catheter system alone was long, and 4.5 min were required to

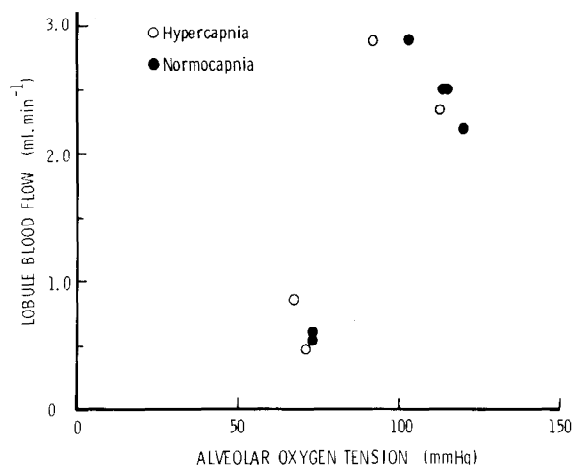


FIG. 7. Experiment 8b. Effect of raised carbon dioxide concentration ($F_{I_{CO_2}}$ 0.078-0.081) on lobule blood flow under normoxic and hypoxic conditions.

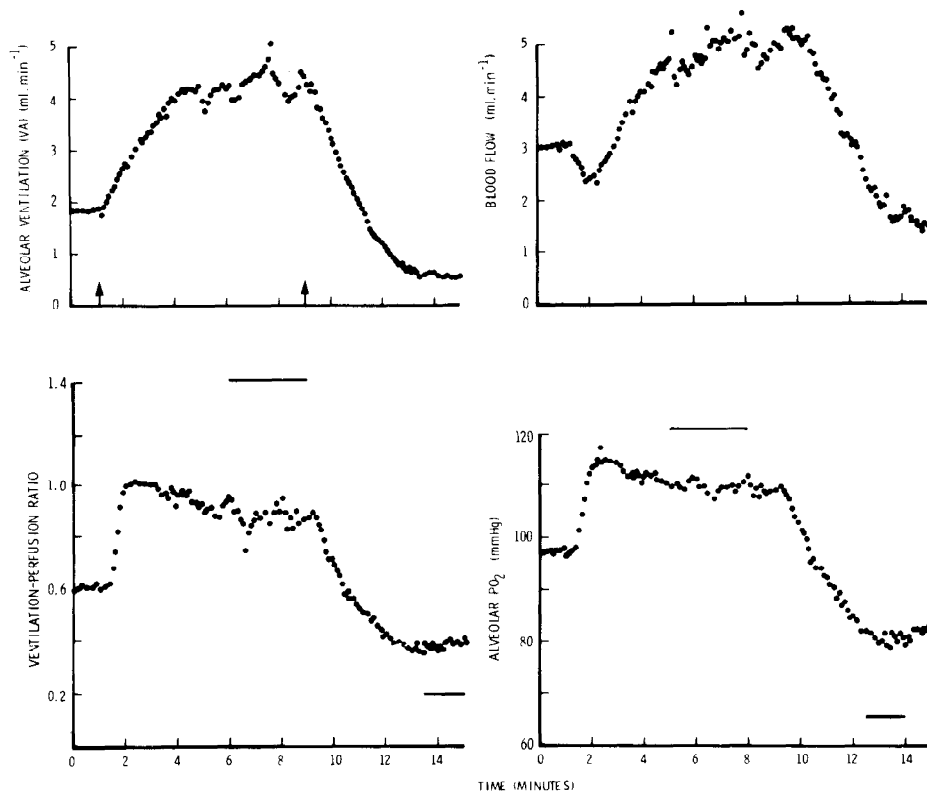


FIG. 8. Experiment 5c. Detailed analysis over a 15-min period of changes of lobule perfusion (Q), ventilation-perfusion ratio (\dot{V}_A/Q), and alveolar oxygen tension ($P_{A_{O_2}}$) as alveolar ventilation (\dot{V}_A) was increased or decreased by changing inspired gas flow rate as indicated by arrows. Continuous lines on \dot{V}_A/Q and $P_{A_{O_2}}$ plots indicate the steady-state values which would have occurred had perfusion remained at the initial value at 0-2 min ($3.02 \text{ ml}\cdot\text{min}^{-1}$).

achieve 95% of the recorded change. Hence step changes of ventilation to assess the speed of response of the local pulmonary circulation could not be made. Nevertheless, the adaptive capacity of the pulmonary circulation is very clearly shown, especially in the difference between the "predicted" and actual P_{O_2} . Had there been no change of perfusion from the initial control value ($3.02 \text{ ml}\cdot\text{min}^{-1}$), \dot{V}_A/\dot{Q} ratio would have increased to 1.41 and later decreased to 0.19, as shown by continuous lines (Fig. 8). Similarly $P_{A_{O_2}}$ would have increased to 122 mmHg (instead of 109.5) and fallen to 66 mmHg (instead of 83.5). The stimulus for these changes is presumably local $P_{A_{O_2}}$ since local $P_{A_{CO_2}}$ changed little throughout (31.7–33.8 mmHg).

Under steady-state conditions (at 1.0, 9.0, and 14.0 min in Fig. 8, for example) regressions of local flow against alveolar oxygen tension were obtained and the data for each experiment is summarized in Table 3. To compare the relationship between local perfusion and $P_{A_{O_2}}$ in different experiments and at different levels of flow, the blood flow at an alveolar oxygen tension of 80 mmHg was calculated from individual regression lines and expressed as a percentage of the flow at 100 mmHg ($\dot{Q}_{80}/\dot{Q}_{100}$). Extrapolation to 100 mmHg was made when necessary. Table 3 shows the range of local blood flow and $P_{A_{O_2}}$ in each experiment, the slope ($\dot{Q}_{80}/\dot{Q}_{100}$) of the relationship between local perfusion and alveolar oxygen tension, and the value of the regression coefficient. As judged by $\dot{Q}_{80}/\dot{Q}_{100}\%$ the oxygen sensitivity of the pulmonary blood vessels varied without obvious reason. There was a correlation with the mixed venous oxygen tension but it was not strong ($r = 0.61$).

CRITICISM OF METHODS

In the first part of this section (A) the physical conditions of the lobules studied are discussed in relation to the surrounding lung; in the second part (B) a systematic examination of the errors and assumptions involved in the calculation of local blood flow is set out.

A. Relationship Between Lobules and Adjacent Lung

1) *Gas mixing between lobule and lung.* Measurements of mixed expired gas from the group of lobules

TABLE 3. Range of measurements of blood flow for whole lung and lobule, lobule alveolar oxygen and carbon dioxide tensions, correlation coefficient, number of measurements, and lobule perfusion

Expt. No.	\dot{Q} (lung), ml·min ⁻¹	\dot{Q} (lob), ml·min ⁻¹	$P_{A_{O_2}}$ (lob), mmHg	$P_{A_{CO_2}}$ (lob), mmHg	r	n	$\dot{Q}_{80}/\dot{Q}_{100}\%$	
2		0.26–1.05	93–118	30–36	0.66	6	39	
3		0.79–3.44	66–89	41–44	0.99	6	51	
5	<i>a</i>	4.97–7.85	95–106	35–36	0.94	5	30	
	<i>b</i>	3.02–4.87	93–110	32–37	0.79	5	57	
7*	<i>a</i>	135–182	0.52–1.44	63–123	11–23	0.94	4	76
	<i>b</i>	182–152	0.34–1.62	71–187	6–22	0.83	5	74
8*	<i>a</i>	198–163	0.66–4.90	54–148	5–36	0.98	8	69
	<i>b</i>	163–154	0.54–2.88	72–120	5–26	0.89	6	59

\dot{Q} (lung) and \dot{Q} (lob) = blood flow for whole lung and lobule; $P_{A_{O_2}}$ (lob) and $P_{A_{CO_2}}$ (lob) = lobule alveolar oxygen and carbon dioxide tensions; r = correlation coefficient for \dot{Q} (lob) against $P_{A_{O_2}}$ (lob); n = no. of measurements; $\dot{Q}_{80}/\dot{Q}_{100}\%$ = lobule perfusion at $P_{A_{O_2}}$ 80 mmHg as a percent of that at 100 mmHg. * Inspired oxygen fraction to lobule varied from 32.5% in *expt 7* to zero in *expt 8*.

under study was not thought to be contaminated with alveolar gas from adjacent lung units because of the striking absence of interlobular collateral gas flow in the coatimundi, as shown in Fig. 9. Alveolar pressure in an isolated coati lung was held constant at +8 cmH₂O while the alveolar pressure of a group of lobules (for the purpose of demonstration, larger than those cannulated *in vivo*) was maintained at -2 cmH₂O with a syringe for over 20 min without change. The alveolar pressure of either "lobule" or lung could be varied independently. In addition, the absence of collateral ventilation was shown *in vivo* because, within the limits of measurement, lobule inspired gas flow equaled mixed expired gas flow. In a similar experiment on a cat, there was no recovery of lobule inspired flow presumably because of escape into adjacent lung units through collateral channels.

2) *Gas diffusion.* Although the lobules in the coati lung are separated from each other by well-defined fibrous septa, diffusion of oxygen and carbon dioxide between the lobules and the surrounding lung would have occurred. Although no experiments were undertaken to assess the importance of tissue diffusion, it is unlikely that diffusion of gases across the boundaries of the region occurred sufficiently rapidly to influence the mean $F_{E_{CO_2}}$, $F_{E_{O_2}}$, and gas R of the lobule, for the following reason. Sequential measurements of mixed expired gases from the lung (breathing air) and the lobule (breathing pure nitrogen) showed that $F_{E_{O_2}}$ from the lobule was 0.0046 when $F_{E_{O_2}}$ (lung) was 0.186, and $F_{E_{CO_2}}$ (lobule) was 0.011 when lung was 0.019. From the gas R values, $P_{A_{O_2}}$ for lobule and lung were 0.275 and 116 mmHg, respectively, and for $P_{A_{CO_2}}$ the values were 0.57 and 27.7 mmHg. This indicates that large gradients of gas concentrations for oxygen and CO₂ could exist between the lobule and the adjacent lung.

3) *Phase differences.* When tidal volumes of whole lung and lobule were compared directly on an oscilloscope, moderate differences in phase were noticed.

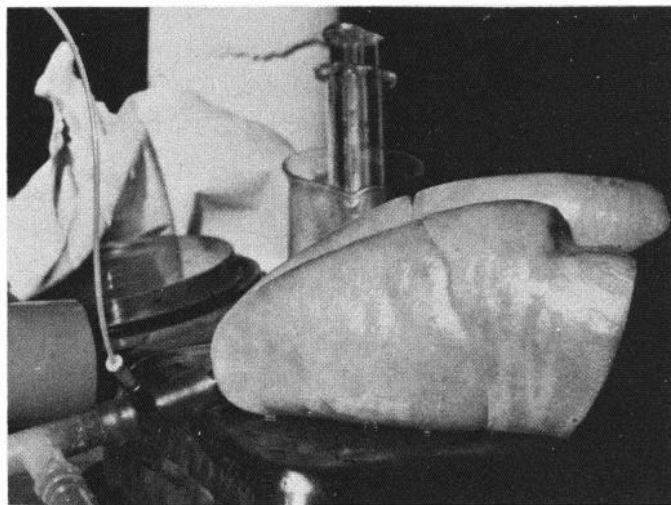


FIG. 9. Excised coati lung inflated with positive pressure (+ 8, cmH₂O) with a blower pump to show absence of collateral flow between subsegments of lower lobe. A group of lobules was cannulated; air was withdrawn with a syringe and the collapsed state maintained at a steady pressure (-2 cmH₂O) for 20 min.

While this was not important in the coati lung from the point of view of collateral ventilation, it undoubtedly set up abnormal mechanical stresses within the lobules and in the lung surrounding them. This might be of importance in regard to the tethering action of lung parenchyma or extra-alveolar vessels and bronchi. Nevertheless, changes of alveolar gas tensions were produced without change of tidal volume. Consequently in any experiment the mechanical situation in the "lobule" remained constant for reasonably long periods of time.

4) *Change of alveolar gas pressure.* Because of the resistance of the tubing, the end pressure at the tip of the catheter was 1 cmH₂O at the highest inspired gas flow (10 ml/min). Such a modest increase in alveolar pressure should not impede local blood flow significantly. In practice, the increase in local alveolar gas pressure with a high inspired gas flow was accompanied by increases, not decreases, in local blood flow.

B. Derivation of Local Blood Flow

1) *Measurement of gas R.* Equation 1, which was used for the calculation of respiratory exchange ratio (see METHODS), assumes no net nitrogen exchange. While this is true in the steady state for the lungs as a whole, nitrogen uptake or excretion may occur in different lung units because of differences between mixed venous and alveolar nitrogen tensions. Nitrogen uptake by the blood is proportional to $\alpha \cdot \dot{Q}(\text{P}_{\text{A}_{\text{N}_2}} - \text{P}\bar{v}_{\text{N}_2})/\text{P}_{\text{tot}}$, where α is the solubility coefficient for nitrogen at atmospheric pressure (0.013), \dot{Q} is local perfusion in ml·min⁻¹, and P_{tot} is the total pressure of dry gases in the alveolar gas. Taking the most extreme example, when the lobule was breathing pure nitrogen, the uptake by the lobule was approximately $0.013 \times 0.2 (716-646)/726$, i.e., 0.00025 ml·min⁻¹. This rate of uptake would have a negligible effect on the alveolar nitrogen concentration or tension or in the calculation of local gas R using Eq. 1.

2) *Measurement of CO₂ production.* Carbon dioxide production (\dot{V}_{CO_2}) was calculated with an approximation equation $\dot{V}_{\text{CO}_2} = (\text{F}_{\text{E}_{\text{CO}_2}} - \text{F}_{\text{I}_{\text{CO}_2}}) \cdot \dot{V}_{\text{I}}$, where \dot{V}_{I} was lobule inspired flow rate in ml·min⁻¹ corrected to STPD. Otis (26) has shown that the error is negligible when $\text{F}_{\text{I}_{\text{CO}_2}}$ is zero. When carbon dioxide was added to the inspired air \dot{V}_{CO_2} was calculated according to Eq. 8 of Otis (26). Oxygen consumption was derived from $\dot{V}_{\text{CO}_2}/\text{R}$. There is also a small error partly dependent on $(1 - \text{R})$ because of the use of \dot{V}_{I} instead of \dot{V}_{E} . For the lowest R value breathing air (0.47) the error was 2.5%, rising to 4.5% when the inspired gas was 30% oxygen ($\text{R} = 0.345$). With hypoxic gas mixtures the proportions of oxygen and carbon dioxide in alveolar gas becomes so small that this error becomes negligible. No correction has been made for the overestimations of \dot{V}_{CO_2} .

3) *Sampling of mixed venous blood.* The P_{O_2} and P_{CO_2} of the blood in the right atrium may not reflect the true mixed venous gas tensions in the pulmonary artery. For technical reasons we were unable to advance the sampling catheter beyond the atrium. Changing $\text{P}\bar{v}_{\text{O}_2}$ to 5 mmHg greater or less than the value actually measured introduced a more or less systematic error into the

measurement of lobule blood flow. For example, in Fig. 6 parallel shifts in the curves were produced with very little change of slope. With $\text{P}\bar{v}_{\text{O}_2} + 5$ mmHg, $\dot{Q}_{80}/\dot{Q}_{100}$ was 0.75, and for $\text{P}\bar{v}_{\text{O}_2} - 5$ mmHg $\dot{Q}_{80}/\dot{Q}_{100}$ was 0.62, compared with 0.69 with the measured $\text{P}\bar{v}_{\text{O}_2}$. The zero flow intercept was 23 mmHg above $\text{P}\bar{v}_{\text{O}_2}$ in the former case, and 12.5 mmHg below $\text{P}\bar{v}_{\text{O}_2}$ in the latter. At $\text{P}_{\text{A}_{\text{O}_2}}$ 100 mmHg absolute flow was 30% greater with $\text{P}\bar{v}_{\text{O}_2} + 5$ mmHg and 20% less with $\text{P}\bar{v}_{\text{O}_2} - 5$ mmHg. Changing $\text{P}\bar{v}_{\text{CO}_2}$ (± 2 mmHg) and pH (± 0.01) had no significant effect.

4) *Alveolar to end-capillary gradients (diffusion).* We assumed that there were no end-capillary gradients for oxygen. With a low alveolar oxygen tension changes in the mixed venous-alveolar P_{O_2} gradient and red cell transit time might have opened up a diffusion gradient. Further discussion on this possibility is beyond the scope of this paper.

5) *Ideal alveolar to mixed end-capillary gradient (\dot{V}_A/\dot{Q}).* Mismatching of ventilation and perfusion within the lobule would cause an underestimation of local perfusion because Cc'_{O_2} calculated from ideal alveolar gas tensions would be higher (and Cc'_{CO_2} lower) than the true mixed end-capillary blood content because of an "alveolar-arterial" gradient for O_2 and CO_2 . For the lung as a whole, calculations of total pulmonary blood flow in experiments 7 and 8 from a) ideal alveolar gas tensions and b) arterial P_{O_2} were compared to assess the effect of inhomogeneity. In 11 measurements the difference in flow averaged 8.5% (range 5–13%). Because of its small size it is unlikely that inhomogeneity in the lobule was greater than that for the whole lung. Therefore we took 8% as the upper limit of flow underestimation due to inhomogeneity.

6) *Oxygen dissociation curve.* Using the human dissociation curve for oxygen with a P_{50} 10 mmHg less than cat or coati, higher values for flow were obtained for a given $\text{P}_{\text{A}_{\text{O}_2}}$, e.g., 66% higher at $\text{P}_{\text{A}_{\text{O}_2}}$ 100 mmHg. This produces a parallel shift of the \dot{Q} - $\text{P}_{\text{A}_{\text{O}_2}}$ relationship shown in Fig. 6, without alteration of $\dot{Q}_{80}/\dot{Q}_{100}$ (0.7 compared with 0.69). The zero flow intercept was displaced 10 mmHg below $\text{P}\bar{v}_{\text{O}_2}$. Variations in the shape of the oxygen dissociation curve (of cat) retaining the same P_{50} did not significantly alter the calculations of flow.

7) *Metabolism of lung tissue.* The notion that gas R = blood R and the use of the Fick equation for blood flow presupposes that the metabolism of lung tissue is negligible compared to the exchange of oxygen and carbon dioxide between alveolar gas and capillary blood. The oxygen consumption for normal lungs (as a percentage of total oxygen consumption) is less than 1% (12) and we have neglected it in the calculations.

8) *Calculation of flow under hypoxic and hypercapnic conditions.* When lobule inspired oxygen fraction was less than 0.11, R (Fig. 5) became high, $\text{P}_{\text{A}_{\text{CO}_2}}$ low, and pH high. Because of the effect of pH on the CO_2 dissociation curve, increasingly lower values of $\text{P}_{\text{A}_{\text{CO}_2}}$ had to be chosen to get the Cc'_{CO_2} low enough for blood R to equal gas R. In the final solution $\text{P}_{\text{A}_{\text{CO}_2}}$ was lower than the measured $\text{P}_{\text{E}_{\text{CO}_2}}$, and \dot{V}_A as derived was many times greater than the measured \dot{V}_{E} . The reason may lie in the differences between pH, P_{CO_2} , and CO_2 content at

very low values of P_{CO_2} in the in vitro and in vivo situations. In addition, within this range of high R values, small errors in its measurement have large effects on the derivation of blood flow. Consequently an alternative method of calculation was used (see Fig. 4) in which a "reasonable" value for alveolar ventilation was assumed. The blood flow calculated by this alternative method when FI_{O_2} was less than 0.105 was 10–23% greater than that calculated in the usual manner (Fig. 4, continuous lines) and was only used in *experiment 8* (Figs. 6 and 7).

When inspired P_{CO_2} was greater than mixed venous P_{CO_2} (Fig. 7), gas R values were so low they failed to intersect the "VA/Q line" between mixed venous and inspired gas points. In this event either $\dot{V}CO_2$ was lower or $\dot{V}O_2$ was higher than expected. Since this occurred under conditions of hypercapnia with hypoxia or normoxia, the lower gas R value was probably related to a low $\dot{V}CO_2$. It is of interest that impaired carbon dioxide uptake with alveolar hypercapnia has been observed before (2, 21, 22) though not in small lung units.

DISCUSSION

Evidence for Hypoxic Vasoconstriction at Sublobar Level

The advantages of this preparation for studying local pulmonary blood flow and gas exchange are clear: *a*) well-developed fibrous septa in the coati lung allowed small units to be studied independently; *b*) continuous measurements of local $\dot{V}A/Q$ and alveolar PO_2 and PCO_2 were available; *c*) mixed venous and arterial blood gas tensions remained undisturbed during changes of local gas tensions; *d*) the animal was breathing spontaneously and had the minimum of surgical interference. On the other hand, the presence of the lobular catheter was a mechanical interference and the method of measuring blood flow was indirect. We have criticized our method for measuring pulmonary blood flow in an earlier section. Even if the assumptions were in error, the evidence that hypoxic vasoconstriction occurs locally is strong.

For example, Fig. 5 shows that lobular carbon dioxide output decreased by more than 50% when inspired oxygen was reduced from 30% to zero. Under these circumstances any mechanical disturbance caused by the lobular catheter would have been constant throughout the experiment. Since lobular total ventilation did not change significantly, the decrease in carbon dioxide output could only be explained by *a*) change in distribution of lobular inspired gas, *b*) reduction of lung tissue carbon dioxide production, or *c*) a reduction of local blood flow. Hypoxia appears to have little effect on the distribution of ventilation in dogs (7) or man (6, 18). The oxygen consumption for normal lungs (as percentage of total oxygen consumption) is less than 1% (12) increasing to about 10% in cases of pulmonary tuberculosis or carcinoma (12, 13) so any changes in lung tissue metabolic rate would be insufficient to explain a fall of 50% in carbon dioxide production. A reduction of local blood flow is the only remaining possibility.

Effect of PA_{O_2} on Local Perfusion

As an index of the oxygen sensitivity of the pulmonary vessels we calculated local flow at an alveolar oxygen tension of 80 mmHg as a percentage of that at 100 mmHg ($\dot{Q}_{80}/\dot{Q}_{100}$, see Table 3). There was a wide range of values from 30 to 76%. The oxygen sensitivity of vessels at a subsegmental level appears to be greater than at the lobar level in dogs or cats (3) with open chest (calculated $\dot{Q}_{80}/\dot{Q}_{100}$ 91%) or with unilateral hypoxia (24) in the dog with closed chest (70%). The response to unilateral hypoxia in awake man is less dramatic. Arborelius (1) found about 14% reduction in unilateral perfusion when one lung was breathing 15% oxygen; extrapolation in terms of $\dot{Q}_{80}/\dot{Q}_{100}$ is difficult but a value of 85–90% would be reasonable. None of these studies mention whether the composition of the mixed venous blood remained constant. All these findings stand out in sharp contrast to those in awake man (11), intact (16) or isolated (8) cat lungs where little or no constriction of pulmonary blood vessels occurred until PA_{O_2} fell to 60 mmHg or less.

There are several aspects of the relationship between subsegmental blood flow and alveolar oxygen tension in the coati lung which differ from other studies of the oxygen sensitivity of the pulmonary vessels in other species such as cats (3) and dogs (24). First, as shown in Fig. 6, local perfusion fell to zero at approximately the level of mixed venous PO_2 , whereas, in lobes of open-chest cats and dogs, flow continued to decrease until zero PA_{O_2} was reached (3). *Experiment 8* was the best and most stable preparation. The extrapolated zero flow point in other experiments varied over quite a wide range (18–71 mmHg) and correlation with $P\bar{V}O_2$ was only fair ($r = -0.61$). Nevertheless, the notion that the caliber of the smaller pulmonary arteries is related to the difference between mixed venous and alveolar oxygen tension is particularly intriguing. Second, a linear increase of pulmonary blood flow with PA_{O_2} up to levels of 150 mmHg (Fig. 6) has not been previously described, although for lobar and unilateral flow Barer et al. (3) and Rahn and Bahnson (28) found increases of flow at PA_{O_2} 150 mmHg relative to that at PA_{O_2} 100 mmHg of 10 and 33%, respectively. Similar changes were found in *experiment 7* at PA_{O_2} 's up to 190 mmHg (Table 3) but in other preparations (breathing air) the highest alveolar oxygen tension achieved was only 120 mmHg. These results imply a considerable degree of local vasomotor tone in the coati lung at PA_{O_2} 100 mmHg. In man there is relatively little vasomotor tone at such PA_{O_2} 's (10) and breathing 100% oxygen does not alter the regional distribution of pulmonary blood flow in the erect position (18) in spite of calculated PA_{O_2} breathing air of about 130 mmHg at the lung apex and 90 mmHg at the base (34). Whether these differences represent a special adaptation of the coati lung to hypoxia is not certain because comparable studies of local pulmonary blood flow have not yet been carried out in other species. The pulmonary arteries in the coati lung appear to be very thick-walled and extensively muscular (D. Heath, personal communication).

Effect of $P_{A_{CO_2}}$ on Local Perfusion

There is general agreement that hypercapnia constricts pulmonary blood vessels (3, 4, 13) but less strongly per mmHg change than hypoxia. Although our data are limited, no constricting effect of local hypercapnia was seen (Fig. 7). In practice, CO_2 cannot contribute much to local regulation of blood flow in regions of alveolar hypoxia; if local \dot{V}_A/\dot{Q} ratio changes from 1 to zero there will be a 60 mmHg change of alveolar PO_2 (from 100 to 40) but only a 6 mmHg change of alveolar PCO_2 . Bergofsky et al. (4) have suggested that the principal site of action of CO_2 may be on the larger vessels; if so, this might explain the lack of effect of local hypercapnia in our preparation.

Effect of Alveolar Gas Tensions on Local Ventilation

At the regional level, as measured with external counting techniques, hypoxia does not alter the distribution of ventilation in anesthetized dogs (7) or man (6, 18). Although this does not exclude changes in distribution within a zone, we have recently found that the shape of the regional washout of radioactive gases in normal subjects is not altered by breathing 11% oxygen (unpublished observations). Local tidal volume and minute ventilation remained constant over a wide range of PA_{O_2} and PA_{CO_2} (Fig. 5) and in general changed in parallel with lung tidal volume and ventilation. At zero inspired oxygen, alveolar P_{CO_2} , fell to <10 mmHg, a level at which bronchiolar or alveolar duct constriction might be expected on the basis of previous data (33). Although we were not monitoring phase changes of tidal volume between lobule and lung, peripheral constriction, if it occurred, was not sufficient to alter tidal volume. At a subsegmental level, mechanical interdependence may have played a part (24). In conclusion, it is unlikely that changes in the distribution of gas within the lobular units contributed significantly to changes of R or carbon dioxide production.

Local Regulation of Alveolar Oxygen Tension and \dot{V}_A/\dot{Q}

Von Euler and Liljestrand suggested that hypoxic pulmonary vasoconstriction may lead to improved conditions for local gas exchange (9) but there have been few attempts to quantitate this. In this section we suggest that local alveolar oxygen tension (PA_{O_2}) and local blood flow (\dot{Q}) form a negative feedback relationship. We then examine the ability of this system to stabilize PA_{O_2} and \dot{V}_A/\dot{Q} when the normal relationships are disturbed by changes in alveolar ventilation. The conditions for gas exchange can be examined by assessing the degree of homeostasis of \dot{V}_A/\dot{Q} ratio when disturbed by a change of alveolar ventilation.

When hypoxic pulmonary vasoconstriction occurs at a sublobar level, a fall of PA_{O_2} actively decreases local blood flow

$$P_{A_{O_2}} \longrightarrow \dot{Q}$$

The solid arrow indicates that a primary decrease of

PA_{O_2} causes a secondary decrease of \dot{Q} . The fall of \dot{Q} in relation to alveolar ventilation increases the \dot{V}_A/\dot{Q} ratio and hence causes an increase of PA_{O_2} which can be verified by inspection of the $O_2 - CO_2$ diagram

$$\dot{Q} \dashrightarrow PA_{O_2}$$

The interrupted arrow indicates that a primary decrease of \dot{Q} leads to a secondary increase of PA_{O_2} . Combination of these two causal relationships (Fig. 10) demonstrates that PA_{O_2} and \dot{Q} form a negative feedback relationship (29).

A measure of homeostasis commonly used is "open-loop gain" (OLG). When considering regulation of PA_{O_2} it can be defined (28) as

$$OLG = \frac{(dPA_{O_2}/d\dot{V}_A) \text{ open}}{(dPA_{O_2}/d\dot{V}_A) \text{ closed}}$$

where $(dPA_{O_2}/d\dot{V}_A)$ open is the change of PA_{O_2} per unit change of alveolar ventilation if hypoxic vasoconstriction did not exist (equivalent to opening the negative feedback loop between PA_{O_2} and \dot{Q} so that hypoxic vasoconstriction would be ineffective); $(dPA_{O_2}/d\dot{V}_A)$ closed is the small change of PA_{O_2} per unit change of \dot{V}_A in the presence of hypoxic vasoconstriction which reduces the change of PA_{O_2} when disturbed by altering \dot{V}_A (closed-loop situation). Clearly if a primary change of PA_{O_2} caused little change of \dot{Q} (i.e., hypoxic vasoconstriction was weak) then $(dPA_{O_2}/d\dot{V}_A)$ closed would tend toward the value of $(dPA_{O_2}/d\dot{V}_A)$ open and OLG would tend to zero. On the other hand, with a high degree of hypoxic vasoconstriction, homeostasis of PA_{O_2} would improve and there would be little change of PA_{O_2} occurring per unit change of alveolar ventilation. $(dPA_{O_2}/d\dot{V}_A)$ closed would tend to zero and OLG toward infinity. For \dot{V}_A/\dot{Q} homeostasis open-loop gain can be defined as

$$OLG = \frac{d(\dot{V}_A/\dot{Q})/d\dot{V}_A \text{ open}}{d(\dot{V}_A/\dot{Q})/d\dot{V}_A \text{ closed}}$$

and similar arguments apply as described above.

OLG can be calculated as the negative of the product of the derivatives of the two causal relationships making up the negative feedback loop. Since the system is nonlinear only small changes of \dot{V}_A were considered at different \dot{V}_A/\dot{Q} ratios. In this way, linear approximations were used without loss of accuracy (28)

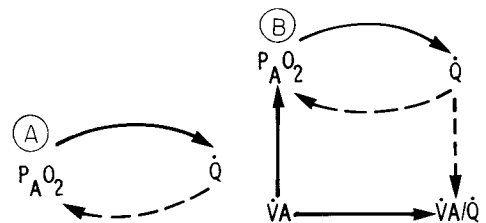


FIG. 10. A: diagram of negative feedback relationship between local alveolar oxygen tension (PA_{O_2}) and local blood flow (\dot{Q}). Continuous line and arrow indicates that a primary decrease of PA_{O_2} causes a secondary decrease of \dot{Q} and interrupted line that a primary decrease of \dot{Q} causes a secondary increase in PA_{O_2} . B: similar convention as in A. Outside the negative feedback loop between PA_{O_2} and \dot{Q} is local alveolar ventilation (\dot{V}_A) which a) can change PA_{O_2} , b) determines (with \dot{Q}) the local ventilation-perfusion ratio (\dot{V}_A/\dot{Q}).

$$\text{OLG} = - \left(\frac{d\dot{Q}}{dP_{A_{O_2}}} \right)_{\dot{V}_A/\dot{Q}} \times \left(\frac{\delta P_{A_{O_2}}}{\delta \dot{Q}} \right)_{\dot{V}_A/\dot{Q}}$$

where subscript \dot{V}_A/\dot{Q} represents the value of the ventilation-perfusion ratio at which the derivative was calculated.

In the APPENDIX we have shown the above expression not only applies to the calculation of OLG when considering the stability of $P_{A_{O_2}}$, which is a member of the negative feedback loop, but also to the calculation of OLG when considering the stability of \dot{V}_A/\dot{Q} which is not a member of the feedback loop (Fig. 10B). At any \dot{V}_A/\dot{Q} ratio, changes of \dot{Q} are expressed as fractional changes so the blood flow, at any \dot{V}_A/\dot{Q} ratio, is considered to be unity. This allows $(d\dot{Q}/dP_{A_{O_2}})_{\dot{V}_A/\dot{Q}}$, which is the first derivative of the relationship describing hypoxic vasoconstriction, to be calculated from the slope of the plot of local blood flow against $P_{A_{O_2}}$ (Fig. 7) divided by the blood flow at a particular $P_{A_{O_2}}$ and \dot{V}_A/\dot{Q} ratio. $(\delta P_{A_{O_2}}/\delta \dot{Q})_{\dot{V}_A/\dot{Q}}$ is the partial derivative of the other relationship of the negative feedback loop ($\dot{Q} \rightarrow P_{A_{O_2}}$). Fractional changes of \dot{Q} were calculated from the following expression

$$\dot{V}_A = \frac{8.63 (Ca_{O_2} - C\bar{v}_{O_2})}{(P_{I_{O_2}} \cdot B - P_{A_{O_2}})}$$

where $P_{I_{O_2}}$ is inspired oxygen tension, B is the inspired-expired volume difference correction factor, $C\bar{v}_{O_2}$ is mixed venous oxygen content, and Ca_{O_2} is arterial oxygen content. An algebraic solution is not possible since this expression describes the solution of two simultaneous equations, i.e., when blood R equals gas R. Differentiation was achieved by a numerical method.²

The relationship between OLG at different values of local $P_{A_{O_2}}$ and \dot{V}_A/\dot{Q} is shown in Fig. 11. The highest OLG occurs close to normal values of $P_{A_{O_2}}$ and \dot{V}_A/\dot{Q} . Data from *experiment 8a* were used because the changes of local blood flow were studied over the widest range of $P_{A_{O_2}}$. The values of $(d\dot{Q}/dP_{A_{O_2}})$ were calculated from Fig. 6. In other experiments over a narrower physiological range of $P_{A_{O_2}}$, the data of OLG plotted against $P_{A_{O_2}}$ and \dot{V}_A/\dot{Q} is less extensive but mean OLG at $P_{A_{O_2}}$ 100 mmHg was 0.82 ranging from 0.5 to 1.21.

From OLG a minimification ratio (M) can be calculated as $1/(1 + \text{OLG})$, where M expressed as a percentage is the diminution of \dot{V}_A/\dot{Q} change compared with a passive system (25). For example, an open-loop gain of 0.5 means that only 66% of the change expected from a passive system without hypoxic vasoconstriction actually occurred. For OLG 1.2, the change was 45% of that expected; with near-perfect control less than 1% change would occur. These values of OLG indicate that hypoxic vasoconstriction reduces changes in \dot{V}_A/\dot{Q} ratio evoked by altering alveolar ventilation to a rather limited extent, and has little effect when the extremes of \dot{V}_A/\dot{Q} are encountered.

Ross et al. (32) looked at the efficiency of local vasodi-

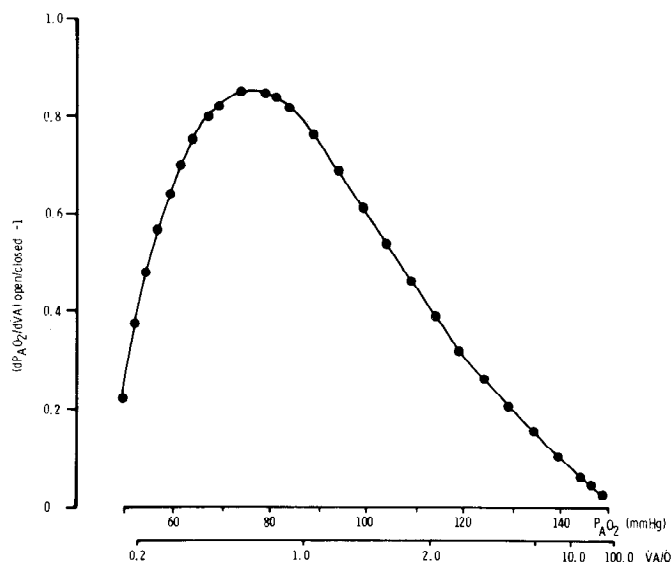


FIG. 11. Open-loop gain plotted against local alveolar oxygen tension ($P_{A_{O_2}}$) and local ventilation-perfusion (\dot{V}_A/\dot{Q}) ratio. Ability of local pulmonary circulation to stabilize $P_{A_{O_2}}$ and \dot{V}_A/\dot{Q} is greatest in the physiological range for both measurements, but is relatively poor outside this range. See text for details.

lation in maintaining a constant level of oxygen availability in the hindlimb of the dog. As arterial oxygen saturation (Sa_{O_2}) was lowered local blood flow increased. The open-loop gain of the system was >10 as Sa_{O_2} fell from 100 to 70% decreasing to 1.0 when Sa_{O_2} was 30%. Although measurements of oxygen availability (oxygen content of blood \times flow) cannot be compared directly with local alveolar P_{O_2} or \dot{V}_A/\dot{Q} ratio, these results suggest that the systemic circulation is better equipped to maintain constant tissue oxygen supply than the pulmonary circulation. Both systems exhibit a decrease in efficiency as oxygen supply is reduced. It is of interest that Fishman (10) concluded that passive influences were more important than vasomotor activity in the regulation of the pulmonary circulation and that alveolar gas tensions contributed only a fine adjustment.

APPENDIX

In the steady state the following relationships can be considered from our symbol-arrow diagram (Fig. 11B)

$$P_{A_{O_2}} = f(\dot{V}_A, \dot{Q}) \quad (1)$$

$$\dot{Q} = f(P_{A_{O_2}}) \quad (2)$$

$$\dot{V}_A/\dot{Q} = f(\dot{V}_A, \dot{Q}) \quad (3)$$

Equation 3 is not required for calculation of OLG when homeostasis of $P_{A_{O_2}}$ is being considered. In these circumstances, there are three variables to be considered ($P_{A_{O_2}}$, \dot{V}_A , \dot{Q}) and it is necessary to find the total differential of $P_{A_{O_2}}$ which can be found in terms of the partial derivatives. Considering a certain point p which is ($P_{A_{O_2}}$, \dot{V}_A , \dot{Q}), we obtain the total differential of Eq. 1 and 2

$$\Delta P_{A_{O_2}} = \left(\frac{\delta P_{A_{O_2}}}{\delta \dot{V}_A} \right)_p \Delta \dot{V}_A + \left(\frac{\delta P_{A_{O_2}}}{\delta \dot{Q}} \right)_p \Delta \dot{Q} \quad (4)$$

$$\Delta \dot{Q} = \left(\frac{\delta \dot{Q}}{\delta P_{A_{O_2}}} \right)_p \Delta P_{A_{O_2}} \quad (5)$$

In the closed-loop condition $\Delta \dot{Q} \neq 0$.

² University of London Computer Centre SSP Library Legrangian interpolation polynomial of 2nd degree employing double-precision argument values.

Substituting $\Delta\dot{Q}$ from Eq. 5 into Eq. 4 and rearranging

$$\left(\frac{\Delta P_{A_{O_2}}}{\Delta \dot{V}_A}\right)_{\text{closed}} = \frac{(\delta P_{A_{O_2}}/\delta \dot{V}_A)_p}{1 - (\delta P_{A_{O_2}}/\delta \dot{Q})_p (d\dot{Q}/dP_{A_{O_2}})_p} \quad (6)$$

When the loop is open $\Delta\dot{Q} = 0$. Therefore from Eq. 1

$$\left(\frac{\Delta P_{A_{O_2}}}{\Delta \dot{V}_A}\right)_{\text{open}} = \left(\frac{\delta P_{A_{O_2}}}{\delta \dot{V}_A}\right)_p \quad (7)$$

By definition

$$\text{OLG} = \left[\frac{(dP_{A_{O_2}}/d\dot{V}_A)_p \text{ open}}{(dP_{A_{O_2}}/d\dot{V}_A)_p \text{ closed}} \right] - 1 \quad (8)$$

By making linear approximations at point p using small changes of \dot{V}_A , $(\Delta P_{A_{O_2}}/\Delta \dot{V}_A)_p$ closed and $(\Delta P_{A_{O_2}}/\Delta \dot{V}_A)_p$ open become $(dP_{A_{O_2}}/d\dot{V}_A)_p$ closed and $(dP_{A_{O_2}}/d\dot{V}_A)_p$ open.

Substituting Eq. 6 and 7 in 8

$$\text{OLG} = (\delta P_{A_{O_2}}/\delta \dot{Q})_p \times (d\dot{Q}/dP_{A_{O_2}})_p$$

The effect of the feedback loop on a variable which is not itself a member of the loop (i.e., \dot{V}_A/\dot{Q} ; see Fig. 10B) may differ from its effect on a loop member (28, p. 329). We now show that the expression derived above for OLG applies for the homeostasis of \dot{V}_A/\dot{Q} as well as $P_{A_{O_2}}$. When considering the homeostasis of \dot{V}_A/\dot{Q} following a disturbance of \dot{V}_A , Eq. 3 must be taken into account. There are now four variables ($P_{A_{O_2}}$, \dot{V}_A , \dot{Q} , \dot{V}_A/\dot{Q}) and linear approximations will be made in a similar manner at point p defined as $(P_{A_{O_2}}$, \dot{V}_A , \dot{Q} , $\dot{V}_A/\dot{Q})_p$.

Obtaining the total differential of Eq. 1, 2, and 3

$$\Delta(\dot{V}_A/\dot{Q}) = \left(\frac{\delta(\dot{V}_A/\dot{Q})}{\delta \dot{V}_A}\right)_p \Delta \dot{V}_A + \left(\frac{\delta(\dot{V}_A/\dot{Q})}{\delta \dot{Q}}\right)_p \Delta \dot{Q} \quad (9)$$

When the loop is closed $\Delta\dot{Q} = 0$.

By combining Eq. 4 and 5 to relate $\Delta\dot{Q}$ to $\Delta\dot{V}_A$, eliminating $P_{A_{O_2}}$, and substituting $\Delta\dot{Q}$ in the resulting expression in Eq. 9 and rearranging, we have

$$\left[\frac{\Delta(\dot{V}_A/\dot{Q})}{\Delta \dot{V}_A} \right]_{\text{closed}} = \left(\frac{\delta(\dot{V}_A/\dot{Q})}{\delta \dot{V}_A} \right)_p + \frac{\left(\frac{\delta(\dot{V}_A/\dot{Q})}{\delta \dot{Q}} \right)_p \cdot \left(\frac{d\dot{Q}}{dP_{A_{O_2}}} \right)_p \cdot \left(\frac{\delta P_{A_{O_2}}}{\delta \dot{V}_A} \right)_p}{1 - \left(\frac{d\dot{Q}}{dP_{A_{O_2}}} \right)_p \cdot \left(\frac{\delta P_{A_{O_2}}}{\delta \dot{Q}} \right)_p} \quad (10)$$

REFERENCES

1. ARBORELIUS, M., JR. Kr⁸⁵ in the study of pulmonary circulation and ventilation during unilateral hypoxia. *Scand. J. Respirat. Diseases Suppl.* 62: 105-108, 1966.
2. ASHTON, C. H., AND G. J. R. MCHARDY. A rebreathing method for determining mixed venous PCO₂ during exercise. *J. Appl. Physiol.* 18: 668-671, 1963.
3. BARER, G. R., P. HOWARD, AND J. W. SHAW. Stimulus-response curves for the pulmonary vascular bed to hypoxia and hypercapnia. *J. Physiol., London* 221: 139-155, 1970.
4. BERGOFKY, E. H., F. HAAS, AND R. J. PORCELLI. Determination of the sensitive vascular sites from which hypoxia and hypercapnia elicit rises in pulmonary artery pressure. *Federation Proc.* 27: 1420-1425, 1968.
5. DAVIES, E. E., H. L. HAHN, G. S. SPIRO, AND R. H. T. EDWARDS. A new technique for recording respiratory transients at the start of exercise. *Respiration Physiol.* 20: 69-79, 1974.
6. DAWSON, A. Regional pulmonary blood flow in sitting and supine man during and after acute hypoxia. *J. Clin. Invest.* 48: 301-310, 1969.
7. DUGARD, A., AND A. NAIMARK. Effect of hypoxia on distribution of pulmonary blood flow. *J. Appl. Physiol.* 23: 663-671, 1967.
8. DUKE, HELEN N. Pulmonary vasomotor responses of isolated perfused cat lungs to anoxia and hypercapnia. *Quart. J. Exptl. Physiol.* 36: 75-88, 1951.
9. EULER, U. S. VON, AND G. LILJESTRAND. Observations on the pulmonary arterial blood pressure in the cat. *Acta Physiol. Scand.* 12: 301-320, 1946.

Since the partial derivatives $(\delta(\dot{V}_A/\dot{Q})/\delta \dot{Q})_p$ and $(P_{A_{O_2}}/\delta \dot{V}_A)_p$ can both be obtained from the equation for \dot{V}_A/\dot{Q}

$$\left(\frac{\delta(\dot{V}_A/\dot{Q})}{\delta \dot{Q}}\right)_p \left(\frac{\delta P_{A_{O_2}}}{\delta \dot{V}_A}\right)_p = \left(\frac{\delta(\dot{V}_A/\dot{Q})}{\delta \dot{V}_A}\right)_p \cdot \left(\frac{\delta P_{A_{O_2}}}{\delta \dot{Q}}\right)_p$$

Therefore by rearranging equation (10) and taking linear approximations

$$\left[\frac{d(\dot{V}_A/\dot{Q})}{d\dot{V}_A} \right]_{\text{closed}} = \left(\frac{\delta(\dot{V}_A/\dot{Q})}{\delta \dot{V}_A} \right)_p + \frac{\left(\frac{\delta(\dot{V}_A/\dot{Q})}{\delta \dot{V}_A} \right)_p \cdot \left(\frac{d\dot{Q}}{dP_{A_{O_2}}} \right)_p \cdot \left(\frac{\delta P_{A_{O_2}}}{\delta \dot{Q}} \right)_p}{1 - \left(\frac{d\dot{Q}}{dP_{A_{O_2}}} \right)_p \cdot \left(\frac{\delta P_{A_{O_2}}}{\delta \dot{Q}} \right)_p} \quad (11)$$

When loop is open $\Delta\dot{Q} = 0$ and Eq. 9 becomes (with linear approximations)

$$\left[\frac{d(\dot{V}_A/\dot{Q})}{d\dot{V}_A} \right]_{\text{open}} = \left(\frac{\delta(\dot{V}_A/\dot{Q})}{\delta \dot{V}_A} \right)_p$$

By definition

$$\text{OLG} = \frac{(d(\dot{V}_A/\dot{Q})/d\dot{V}_A)_{\text{open}}}{(d(\dot{V}_A/\dot{Q})/d\dot{V}_A)_{\text{closed}}}$$

Substituting Eq. 11 and 12 in this expression for OLG and simplifying we have

$$\text{OLG} = \left(\frac{\delta P_{A_{O_2}}}{\delta \dot{Q}} \right)_p \left(\frac{d\dot{Q}}{dP_{A_{O_2}}} \right)_p$$

The idea for this project was suggested by Professor J. Mead while J. M. B. Hughes was working as a Dorothy Temple Cross MRC Research Fellow, in the Dept. of Physiology at the Harvard School of Public Health, Boston, Mass. Pilot experiments, without mass spectrometer sampling, were carried out in that laboratory with Dr. F. G. Hoppin, Jr., and Dr. D. Leith who also designed the lobule spirometer (with assistance from Mr. N. Petersen). We are grateful to Professor G. R. Kelman for advice about gas-exchange computer analysis and to Mr. J. Dolan for assistance in writing the \dot{V}_A/\dot{Q} program. Miss A. Hart and Miss K. Patel gave valuable technical assistance.

Received for publication 5 May 1975.

10. FISHMAN, A. P. Respiratory gases in the regulation of the pulmonary circulation. *Physiol. Rev.* 41: 214-280, 1961.
11. FISHMAN, A. P., A. HIMMELSTEIN, H. W. FRITTS, AND A. COURNAND. Blood flow through each lung in man during unilateral hypoxia. *J. Clin. Invest.* 34: 637-646, 1955.
12. FRITTS, H. W., JR., D. W. RICHARDS, AND A. COURNAND. Oxygen consumption of tissues in the human lung. *Science* 133: 1070-1072, 1961.
13. FRITTS, H. W., JR., B. STRAUSS, W. WICHERN, AND A. COURNAND. Utilization of oxygen in the lungs of patients with diffuse non-obstructive pulmonary disease. *Trans. Assoc. Am. Physicians* 76: 302-311, 1963.
14. GOMEZ, D. M. Considerations of oxygen-hemoglobin equilibrium in the physiological state. *Am. J. Physiol.* 200: 135-142, 1961.
15. GUYTON, A. C., C. E. JONES, AND T. G. COLEMAN. In: *Circulatory Physiology: Cardiac Output and Its Regulation*. Philadelphia, Pa.: Saunders, 1973.
16. HAUGE, A., AND N. C. STAUB. Prevention of hypoxic vasoconstriction in cat lung by histamine-releasing agent 48/80. *J. Appl. Physiol.* 26: 687-698, 1969.
17. HERTZ, C. W. Untersuchungen über den Einfluss der alveolaren Gasdrücke auf die intrapulmonale Durchblutungsverteilung beim Menschen. *Klin. Wochschr.* 34: 472-477, 1956.
18. HOLLEY, H. S., A. DAWSON, A. C. BRYAN, J. MILIC-EMILI, AND D. V. BATES. Effect of oxygen on the regional distribution of ventilation and perfusion in the lung. *Can. J. Physiol. Pharmacol.* 44: 89-93, 1966.

19. KATO, M., AND N. C. STAUB. Response of small pulmonary arteries to unilobar hypoxia and hypercapnia. *Circulation Res.* 19: 426, 1966.
20. KELMAN, G. R. Computer program for the production of O₂-CO₂ diagrams. *Respiration Physiol.* 4: 260-269, 1968.
21. KROGH, A. On the mechanism of the gas-exchange in the lungs. *Scand. Arch. Physiol.* 23: 248-278, 1910.
22. LASZLO, G. *Alveolar Carbon Dioxide Pressures in the Unsteady State* (M. D. thesis). University of Cambridge, 1971.
23. LINDEN, R. J., J. R. LEDSOME, AND J. NORMAN. Simple methods for the determination of the concentrations of CO₂ and O₂ in blood. *Brit. J. Anaesthesia* 37: 77-88, 1965.
24. MEAD, J., T. TAKISHIMA, AND D. LEITH. Stress distribution in lungs: a model of pulmonary elasticity. *J. Appl. Physiol.* 28: 596-608, 1970.
25. MILHORN, H. T. In: *The Application of Control Theory to Physiological Systems*. Philadelphia, Pa.: Saunders, 1966.
26. OTIS, A. B. Quantitative relationships in steady-state gas exchange. In: *Handbook of Physiology. Respiration*. Washington, D. C.: Am. Physiol. Soc., 1964, sect. 3, vol. 1, chapt. 27, p. 681-698.
27. RAHN, H. A concept of mean alveolar air and the ventilation-blood flow relationships during pulmonary gas exchange. *Am. J. Physiol.* 158: 21-30, 1949.
28. RAHN, H., AND H. T. BAHNSON. Effect of unilateral hypoxia on gas exchange and calculated pulmonary blood flow in each lung. *J. Appl. Physiol.* 6: 105-112, 1953.
29. RIGGS, D. S. Feedback: fundamental relationship or frame of mind? *Advan. Enzyme Regulation* 5: 357-382, 1967.
30. RIGGS, D. S. In: *Control Theory and Physiological Feedback Mechanisms*. Baltimore, Md.: Williams & Wilkins, 1970, p. 332.
31. RILEY, R. L., AND A. COURNAND. "Ideal" alveolar air and the analysis of ventilation-perfusion relationships in the lungs. *J. Appl. Physiol.* 1: 825-847, 1949.
32. ROSS, J. M., H. M. FAIRCHILD, J. WELDY, AND A. C. GUYTON. Autoregulation of blood flow by oxygen lack. *Am. J. Physiol.* 202: 21-24, 1962.
33. SEVERINGHAUS, J. W., E. W. SWENSON, T. N. FINLEY, M. T. LATEGOLA, AND J. WILLIAMS. Unilateral hypoventilation produced in dogs by occluding one pulmonary artery. *J. Appl. Physiol.* 16: 53-60, 1961.
34. WEST, J. B. Regional differences in gas exchange in the lung of erect man. *J. Appl. Physiol.* 17: 893-898, 1962.

